Ab Initio Studies of Proton Sponges. 2. 1,6-Diazabicyclo[4.4.4]tetradecane

S. T. Howard* and J. A. Platts

Department of Chemistry, University of Wales, P.O. Box 912, Cardiff CF1 3TB, U.K.

R. W. Alder

School of Chemistry, University Of Bristol, Cantock's Close, Bristol BS8 1TS, U.K.

Received December 23, 1994[⊗]

The structures of 1,6-diazabicyclo[4.4.4]tetradecane and its inside-protonated cation have been determined by *ab initio* geometry optimization. The title compound possesses D_3 symmetry in the gas phase; an N···N distance of 2.87 Å is obtained at the Hartree–Fock/6-31G** level of theory. Asymmetric protonation at one nitrogen (lowering the symmetry to C_3) is energetically preferred to the symmetric D_3 $[N\cdots H\cdots N]^+$ bridged form by some 11 kJ mol^{-1}, in contrast to the situation in the solid state and in solution. However, the presence of a barrier to proton transfer between nitrogens is in agreement with numerous theoretical studies on the $[NH_4\cdots NH_3]^+$ cation and on 1,8-bis(dimethylamino)naphthalene. The proton affinity, which has so far proved impossible to measure experimentally, is predicted to be 1088 kJ mol^{-1}, the highest known value for a neutral organic base. A topological analysis of the electron distribution reveals that the two nitrogens are linked by a (3,−1) critical point with a small positive value of $\nabla^2\varrho$, characteristic of a closed-shell interaction. Bond path analysis indicates that there is relief of strain in the C–C bonds on protonation.

Introduction

In a previous paper,[1] which we shall refer to as Paper 1, we studied the archetypal "proton sponge" 1,8-bis(dimethylamino)naphthalene (DMAN) using *ab initio* calculations. This class of compounds characteristically form ionic complexes with a cationic hydrogen bond $[N-H\cdots N]^+$ or $[N\cdots H\cdots N]^+$, and have exceptional basic strength for organic bases due to the proximity of amino groups.[2,3] It is anticipated that the title compound illustrated in Figure 1a, which we shall denote as [4.4.4], is an even stronger base than DMAN. On the basis of molecular mechanics calculations, it has been estimated that the pK_a value may be as high as 25,[4] but it is impossible to verify this experimentally since the proton cannot be inserted by normal proton-transfer reactions and cannot be removed without destroying the molecule. Whilst the pK_a is very difficult to predict theoretically with any accuracy, the proton affinity (PA) is readily accessible with quantum mechanical calculations if the problem can be tackled at a reasonable level of theory. Hence a major aim of this study is to establish the PA of [4.4.4] using Hartree–Fock calculations with gradient-based optimizations.

The crystal and molecular structure of [4.4.4] has been determined by X-ray diffraction.[5] Perhaps surprisingly, the crystal structure of [4.4.4] reveals a highly symmetric molecule with D_3 symmetry and two nitrogen lone pairs (LPs) which point directly toward one another. It is of course possible that the strain energy that this causes is absorbed by relaxation of crystal-packing forces, so the presence of D_3 symmetry in the free base is an open question and one which we have to answer en route to computing the PA. Crystal structures are available for the cation $[4.4.4]H^+$, including both "inside-protonated"[5] (i.e., the proton is inside the cage) and "outside-protonated" forms.[6] Due to the relief of strain and to the hydrogen bonding in the protonated ion, the larger PA is anticipated for the inside-protonated [4.4.4], and in this work we have studied only this form. Like the parent molecule [4.4.4], the reported inside-protonated $[4.4.4]H^+$ structure *in the solid state* effectively has D_3 symmetry. (In this particular salt, Cl^- is the counter-anion.) The study of DMAN in Paper 1 and theoretical studies of proton-bound dimers such as $[NH_4\cdots NH_3]^+$ indicate that asymmetric protonation tends to be energetically preferred.[7,8,9] The crystal structure of the $N_2H_7^+$ cation in the adduct of NH_3 with $NH_4^+I^-$ also has an asymmetric cation.[10] However, earlier calculations by Scheiner[11] showed that, as the N···N distance is reduced, there comes a point where the potential energy surface (PES) becomes a single well. The question of a single-, or double-minimum potential well for proton transfer in $[4.4.4]H^+$ has been discussed before by Alder, Moss, and Sessions.[12] A combination of NMR and IR data strongly suggested that inside-protonated DBT has a single-minimum well (i.e., is centrally, symmetrically protonated) in solution. Here we address whether this is also true in the gas phase.

[⊗] Abstract published in *Advance ACS Abstracts,* June 15, 1995.

(1) Platts, J. A.; Howard, S. T.; Woźniak, K. *J. Org. Chem.* **1994**, *59*, 4647.

(2) Alder, R. W. *Chem. Rev.* **1989**, *89*, 1215.

(3) Staab, H. A.; Saupe, T. *Angew. Chem., Int. Ed. Engl.* **1988**, *27*, 865.

(4) Alder, R. W. Unpublished calculations.

(5) Alder, R. W.; Orpen, A. G.; Sessions, R. B. *J. Chem. Soc., Chem. Commun.* **1983**, 999. For a correction to the space group see: Schaefer, W. B.; Marsh, R. E. *J. Chem. Soc., Chem. Commun.* **1984**, 1555.

(6) Alder, R. W.; Orpen, A. G.; White, J. M. Unpublished. See also: Alder, R. W. *Tetrahedron* **1990**, *46*, 683.

(7) Del Bene, J. E.; Frisch, M. J.; Pople, J. A. *J. Phys. Chem.* **1985**, *89*, 3669.

(8) Ikuta, S. *J. Chem. Phys.* **1987**, *87*, 1900.

(9) Platts, J. A.; Laidig, K. E. *J. Phys. Chem.* **1995**, *99*, 6487.

(10) Berthold, H. J.; Preibsch, W.; Vonholdt, E. *Angew. Chem., Int. Ed. Engl.* **1988**, *27*, 1524.

(11) Scheiner, S. *J. Phys. Chem.* **1982**, *86*, 376.

(12) Alder, R. W.; Moss, R. E.; Sessions, R. B. *J. Chem. Soc., Chem. Commun.* **1983**, 1000.

0022-3263/95/1960-6085$09.00/0

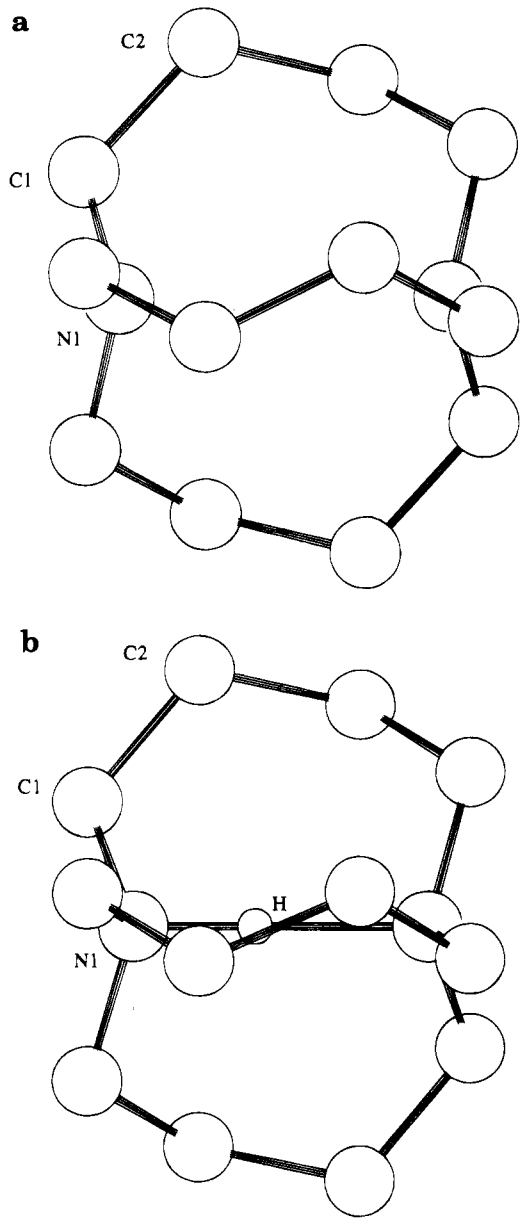

Figure 1. (a) HF/6-31G**-optimized structure of [4.4.4]. (b) HF/6-31G**-optimized structure of [4.4.4]H^+(ii).

Computational Methods

Ab initio calculations employed GAMESS[13] running on DEC Alpha RISC workstations. Direct SCF methods and cutoffs were applied in both geometry optimizations and single-point calculations. The free base and inside-protonated cation were optimized with three different basis sets: STO-3G,[14] 6-31G,[15] and finally 6-31G**.[16] Some 6-31G*//6-31G[16a] calculations have also been performed in order to obtain electron density properties and PAs which are directly comparable with results reported in Paper 1. Restricted Hartree–Fock (RHF) optimizations employed Baker's algorithm.[17] Structures were considered to be optimized when the maximum force on any nucleus did not exceed 10^{-4} au and the root-mean-square force on the nuclei was below one-third of this value.

Geometry optimization of [4.4.4] began with the 6-31G basis set and nuclear coordinates from the crystal structure determination, imposing D_3 symmetry. Taking this optimized structure, it was decided to explore whether the base could have lower (C_2) symmetry, since this would allow the nitrogen LPs to point away from one another. A further optimization with the 6-31G basis set started with such a perturbed C_2 structure, generated from the D_3-optimized structure by moving the nitrogens slightly away from the (former) C_3 axis in opposite directions. After a few steps of optimization, the structure had regained its original D_3 symmetry. This suggests that the D_3 structure is *at least* a local minimum, and given that (i) an STO-3G//STO-3G frequency calculation (reported later) gave no imaginary frequencies and (ii) the experimental (solid-state) structure also has this symmetry, it is likely to be the global minimum energy structure.

Nevertheless, at the 6-31G level we had not eliminated the possibility that a C_1 structure with no symmetry could have the lowest energy. Consequently, starting with the 6-31G D_3-optimized structure we made random perturbations to the positions of all heavy atoms by some 0.1 Å and reoptimized, with the result that the molecule regained D_3 symmetry. Repeating this with a different set of atom shifts, we recovered the same result. The final optimization with the 6-31G** basis set therefore assumed D_3 symmetry.

Initially the 6-31G geometry optimization of [4.4.4]H^+ was also constrained to have D_3 symmetry, with the proton symmetrically positioned at the intersection of the C_3 and three C_2 axes, equidistant from the two nitrogens. The 6-31G-optimized [4.4.4] structure was used as the starting point. Next, the D_3 symmetry constraint was lowered to C_3, thus allowing the proton to move toward one nitrogen along the C_3 axis, and further optimization within the 6-31G basis set was carried out. Two no-symmetry (C_1) initial structures were also considered, in which the proton was displaced 0.1 Å perpendicular to the N···N axis (i) in the mean plane of one butyl arm and (iii) in between two arms. The same result was found: the higher C_3 symmetry was regained. Having obtained 6-31G-optimized structures for both the symmetric D_3-constrained cation (which we shall call [4.4.4]H^+(i)) and the asymmetric C_3 cation ([4.4.4]H^+(ii)), these structures were finally optimized with the larger 6-31G** basis set.

As in the study of DMAN, the computation of a zero-point energy (ZPE) correction to the PA for such large molecules is a major computational task, even with the split-valence 6-31G basis set. Consequently, we must resort to minimal basis set STO-3G calculations of harmonic vibrational frequencies in order to estimate the ZPE correction, suitably scaled in the light of differences between STO-3G and 6-31G** ZPEs in some smaller amines. Optimizations with this basis set resulted in D_3 minimum energy structures for both [4.4.4] *and* [4.4.4]H^+, i.e., the smallest basis set prediction is qualitatively different for the cation. No imaginary frequencies were found for either the free base or cation, verifying that they represent true minimum energy structures at this level of theory.

Critical point (CP) analysis of the electron distribution $\varrho(\mathbf{r})$ and $\nabla^2\varrho(\mathbf{r})$ have again been applied to monitor the changes in electronic structure caused by protonation. This includes a determination of the LP properties, as characterized at the appropriate (3,−3) CP in $-\nabla^2\varrho$. These analyses employed the programs SADDLE and BUFFALO, part of the suite of AIMPAC programs.[18] Relief of strain on protonation is expected to contribute toward the high basicity of [4.4.4]; we therefore report an analysis of the bond path trajectories; these are the lines of maximum electron density joining the nuclei.[19]

(13) Schmidt, M. W.; Baldridge, K. K.; Boatz, J. A.; Elbert, S. T.; Gordon, M. S.; Jensen, J. H.; Koseki, S.; Matsunaga, N.; Nguyen, K. A.; Su, S. J.; Windus, T. L.; Dupuis, M.; Montgomery, J. A. *J. Comput. Chem.* **1993**, *14*, 1347.

(14) Hehre, W. J.; Stewart, R. F.; Pople, J. A. *J. Chem. Phys.* **1969**, *51*, 2657.

(15) (a) Hehre, W. J.; Ditchfield, R.; Pople, J. A. *J. Chem. Phys.* **1972**, *56*, 2257. (b) Ditchfield, R.; Hehre, W. J.; Pople, J. A. *J. Chem. Phys.* **1971**, *54*, 724.

(16) Hariharan, P. C.; Pople, J. A. *Theoret. Chim. Acta* **1973**, *28*, 213.

(17) Baker, J. *J. Comput. Chem.* **1986**, *7*, 385.

(18) Atoms In Molecules Package. Biegler-König, F. W.; Bader, R. F. W.; Tang, T. *J. Comput. Chem.* **1982**, *3*, 317. Latest releases incorporate the programs SADDLE and BUFFALO, which may be obtained from Prof. Richard Bader, McMaster University, Hamilton, Ontario, Canada; E-mail: Bader@ca.mcmaster.cis.mcmail.

(19) Bader, R. F. W. *Atoms In Molecules; A Quantum Theory*; Oxford University Press: Oxford, 1990.

Table 1. Selected Geometrical Parameters (Å and deg)

parameter	[4.4.4] (HF/6-31G**)	[4.4.4] (expt)[a]	[4.4.4]H$^+$ [b] (HF/6-31G**)	[4.4.4]H$^+$ (expt)[a]
r(N1−C1)	1.444	1.443	1.483	1.486
r(C1−C2)	1.534	1.518	1.531	1.515
r(C2−C2′)	1.540	1.519	1.541	1.533
C1−N1−C1″	115.9	115.5	112.7	113.6
N1−C1−C2	114.9	114.1	113.3	112.6
C1−C2−C2′	116.6	116.4	115.9	115.7
C1−N1···N1′	101.9	102.4	106.0	104.9
r(N1···N2)	2.871	2.807	2.521	2.527
r(N1···H$^+$)			1.261	1.263

[a] Reference 5.

The limiting value of the angle subtended at a nucleus where two bond paths meet is known as the "bond path angle".[19] The difference between this angle and the geometrical bond angle has been used to quantify bond strain in molecules such as cyclopropane: a positive value of $(\alpha_b - \alpha_e)$ is generally indicative of strain.

Results and Discussion

D_3 symmetry optimization in the 6-31G basis set gave a free base structure in good general agreement with the crystal structure,[5] but the N···N bridgehead distance was some 0.19 Å larger. Subsequent optimization with the 6-31G** basis set reduced this discrepancy to 0.06 Å (see Figure 1 for a view of the optimized geometry). Table 1 compares some selected bond lengths and bond angles for the HF/6-31G**-optimized structures of [4.4.4], [4.4.4]-H$^+$(i), and the solid-state geometries obtained from X-ray diffraction.[5] In [4.4.4], the mean bond length discrepancy between theory and experiment (taken over the C−C and C−N bonds) is 0.013 Å, and the mean bond angle discrepancy is 0.5°. The nonbonded angle N1′···N1−C1, which effectively measures the degree of pyramidality at the nitrogen atom, is also in agreement between observation and theory (0.5° difference). Thus the *ab initio* calculation generally gives an excellent representation of the molecular geometry (perhaps with some reservations about the N···N distance, since this has been considered to be a key parameter controlling the basic strength in proton sponges).

Table 1 also contains selected geometrical data for the inside-protonated [4.4.4]H$^+$Cl$^-$ complex.[5] The agreement between the theoretical cation D_3-constrained structure [4.4.4]H$^+$(i) and this solid-state experimental structure is excellent. In particular, the N···N distances differ by only 0.006 Å. Bond lengths between heavy atoms show a mean experiment−theory discrepancy of only 0.009 Å, and the mean difference in bond angles is only 0.4°. This level of agreement is rather better than was obtained for DMAN in Paper 1. We attribute this to (i) the larger basis set and (ii) the lesser influence of the counter-ion on the structure of an inside protonated cation.

Breaking the D_3 symmetry to generate [4.4.4]H$^+$(ii) causes little change in the geometry of the cation, except in the N−H···N region, and there is also no experimental structure with which to compare it. Hence we shall not report the geometry of [4.4.4]H$^+$(ii) in similar detail. Instead, we give some key results. The hydrogen bond distances in [4.4.4]H$^+$(ii) are r(N1−H$^+$) = 1.053 Å and r(N2−H$^+$) = 1.576 Å. Hence the N···N distance of 2.628 Å is ≈0.1 Å larger than in [4.4.4]H$^+$(i). The N−C bond lengths show a large left−right (i.e., around different nitrogens) asymmetry (1.474 and 1.490 Å), and so, too, the C−N−C angles (113.6 and 107.0°). Other geometrical results, such as C−C bond lengths and N′···N−C angles, hardly differ between [4.4.4]H$^+$(i) and [4.4.4]H$^+$(ii), and the left−right asymmetry is much less pronounced. The energy difference between forms [4.4.4]H$^+$(i) and [4.4.4]-H$^+$(ii) is 11 kJ mol^{-1} at the 6-31G**/6-31G** level (15 kJ mol^{-1} at the 6-31G*//6-31G level). The second figure may be compared with the value of 22 kJ mol^{-1} found in Paper 1 for 1,8-bis(dimethylamino)naphthalene.

Table 2. Amine PAs and ZPE Corrections (kJ mol^{-1})

	ZPE correction			
	STO-3G	6-31G	6-31G**	6-31G**//6-31G**
ammonia	42.4	45.9	42.5	876.4 (866.1)
methylamine	40.5	44.8	41.2	912.2 (907.9)
dimethylamine	39.5	44.6	43.0	950.0 (939.3)
trimethylamine	38.5	44.1	43.5	969.1 (960.2)

[a] Experimental PAs at 600 K (ref 1) in parentheses.

Table 3. Predicted Proton Affinity of [4.4.4]

	free base energy (hartrees)	cation energy[a] (hartrees)	ΔZPE (kJ mol^{-1})	PA (kJ mol^{-1})
STO-3G//STO-3G	−570.397130	−570.928497	39.8	1355
6-31G//6-31G	−576.984112	−577.425409		1114[b]
6-31G*//6-31G	−577.237425	−577.666703		1082[b]
6-31G**//6-31G**	−577.275392	−577.708411		1088[b,c]

[a] Cation values refer to the asymmetric C_3 form [4.4.4]H$^+$(ii), except in the STO-3G case, where the minimum energy geometry has D_3 symmetry. [b] Including an esdtimated ZPE correction of 45 kJ mol^{-1}. [c] Including a counterpoise correction of 4 kJ mol^{-1}.

Table 4. Lone Pair Properties in [4.4.4] and Monoamines[a]

	ϱ_c (e bohr^{-3})	$\nabla^2\varrho_c$ (e bohr^{-5})	r_c (bohr)
ammonia	0.584	−3.210	0.733
methylamine	0.595	−3.347	0.731
dimethylamine	0.603	−3.441	0.730
trimethylamine	0.608	−3.508	0.729
triethylamine	0.577	−3.033	0.735
[4.4.4]	0.608	−3.440	0.728

[a] At the 6-31G**//6-31G** level.

In Table 2 we report ZPE corrections to the PA for a number of monoamines, computed with STO-3G, 6-31G, and 6-31G** basis sets. The PAs at the 6-31G** level are also reported. The STO-3G basis set consistently underestimates the ZPE correction (compared to the larger basis set) by an amount which varies from 0.1 to 5 kJ mol^{-1}. Taking the trimethylamine cation as the most realistic model for [4.4.4]H$^+$(ii) suggests that the 6-31G** ZPE correction for this cation would be ≈45 kJ mol^{-1}.

Applying the estimated ZPE correction of 45 kJ mol^{-1} appropriately (see Table 3), we therefore obtain a PA *at 0 K* for inside-protonation of [4.4.4] of 1092 kJ mol^{-1}. The 6-31G**/6-31G** PA appearing in Table 3 has been further corrected for basis set superposition error (BSSE) with the usual counterpoise method of Boys and Bernardi[20] (this lowers the PA by 4.3 kJ mol^{-1}). Hence our final calculated PA is 1088 kJ mol^{-1}. The 6-31G**//6-31G** PA for constrained symmetric D_3 protonation is correspondingly 1081 kJ mol^{-1} (without any BSSE correction), i.e., a barrier of 11 kJ mol^{-1} for proton transfer is predicted in [4.4.4]H$^+$(ii).

Surprisingly, given that there are significant differences between 6-31G- and 6-31G**-optimized structures, the 6-31G*//6-31G PA differs by only 10 kJ mol^{-1} from

(20) Boys, S. F.; Bernardi, F. *Mol. Phys.* **1970**, *19*, 553.
(21) Bader, R. F. W.; Essen, H. *J. Chem. Phys.* **1984**, *80*, 1943.

Table 5. Critical Point Analyses of ϱ^a

CP between	CP type	ϱ_c (e bohr^{-3})		$\nabla^2\varrho_c$ (e bohr^{-5})		ϵ	
		[4.4.4]	[4.4.4]H$^+$	[4.4.4]	[4.4.4]H$^+$	[4.4.4]	[4.4.4]H$^+$
N1−C1	(3,−1)	0.283	0.255	−0.960	−0.726	0.044	0.029
C1−C2	(3,−1)	0.257	0.257	−0.688	−0.686	0.033	0.022
C2−C2′)	(3,−1)	0.250	0.249	−0.651	−0.643	0.003	0.004
N1···N1′)	(3,−1)	0.018		+0.050			
(RING)	(3,+1)	0.008	0.011	+0.037	+0.062		
N1−H$^+$	(3,−1)		0.177		−0.497		0.000
H$^+$−N1′	(3,−1)		0.177		−0.497		0.000

[a] At the 6-31G**//6-31G** level. Cation values refer to the D_3 form [4.4.4]H$^+$(i).

the 6-31G**/6-31G** result. The same is generally true on comparing PAs predicted at the same two levels of theory for the series $H_{3-n}NMe_n$, $n = 0, 3$ (compare Table 2 of this work and Table 4 of Paper 1). This suggests two important ideas: (i) the geometry predictions of modest split-valence basis sets are apparently quite adequate for PA calculations, although polarization functions are important in obtaining a reasonable estimate at these geometries, and, perhaps more controversially, (ii) the N···N distance *may not* be such a crucial parameter in determining proton sponge basicity, since the 6-31G N···N distance prediction was 0.18 Å too large (compared to the crystal structure).

Atoms which formally bear a LP invariably have a (3,−3) CP in $-\nabla^2\varrho$ in their valence shell. This effectively locates the LP, as it is the point at which charge is most concentrated.[22] Recent theoretical studies on protonation[23,24] have examined the relationship between the charge density properties at this point and the PA: in monoamines it is found to be a good PA "indicator". A search of $\nabla(\nabla^2\varrho)$ around the nitrogen valence shell of [4.4.4] successfully located the (3,−3) CP. We report two sets of values for ϱ_c and $\nabla^2\varrho_c$: at the 6-31G*//6-31G level and at the 6-31G**//6-31G** level (Table 4). For comparison, LP properties for ammonia, methylamine, dimethylamine, trimethylamine, and triethylamine at the 6-31G**//6-31G** level are also reported. Analogous 6-31G*//6-31G calculations and CP analyses were reported in Table 3 of Paper 1. It is apparent that the nitrogen LP in [4.4.4] has properties close to those of trimethylamine, which has a much lower PA. Therefore like in DMAN, this shows that the very high basicity of [4.4.4] is not due to exceptional electronic structure associated with the nitrogen atom and therefore must have its origin in some other effect, such as the cooperative action of both nitrogens and/or relief of strain.

The CP analysis of ϱ for [4.4.4] and [4.4.4]H$^+$(i) is presented in Table 5. The total charge density ϱ_c, the Laplacian of the charge density $\nabla^2\varrho_c$, and the ellipticity at (3,−1) CPs are reported. Where we may have expected to find a (3,+3) or "cage" CP, a local minimum, there is in fact a (3,−1) or "bond" CP at the origin (midway between the nitrogens) that has typical properties associated with a closed-shell interaction between the nitrogen atoms: a low value of ϱ and positive $\nabla^2\varrho$. The identification of this interaction as a "bond" is arbitrary; Cioslowski has found such CPs in situations which are clearly repulsive, e.g., between hydrogen atoms in biphenyl.[25] Thus, perhaps we can only say with certainty that the nitrogens are interacting via a shared interatomic surface. The presence of a "bond" CP rather than a ring or cage CP at this point means that the interaction is dominated by two (nitrogen) atoms, which is not surprising since they are the nearest atoms and must have a large LP−LP repulsive interaction. On searching ϱ for 1,8-bis(dimethylamino)naphthalene, we also find a (3,−1) CP on the C_2 axis between nitrogens, with an N−CP−N angle of 173.4° and very similar density properties (ϱ_c = 0.0163 e Bohr^{-3}; $\nabla^2\varrho_c$ = +0.056 e Bohr^{-5}; ϵ = 0.26) to the analogous CP in [4.4.4], given in Table 5. In each of the three "arms" of [4.4.4] and [4.4.4]H$^+$ is a (3,+1) "ring" CP, symmetrically placed at the center of each N−C−C−C−C−N ring. As the ring contracts on protonation, ϱ_c and $\nabla^2\varrho_c$ increase at these points (Table 5). The ellipticities {ϵ} (which measure the degree of double-bond character) are small in the C−N and C−C bonds of [4.4.4], becoming even smaller in the cations.

The CP analysis for the charge density of [4.4.4]H$^+$(i) shows large changes in the connecting C−N bonds on protonation, with a large depletion of charge (relative to [4.4.4]) at the bond CP. Changes in the properties of the C−C bonds on protonation are almost negligible. The large value of ϱ_c and the negative value of $\nabla^2\varrho_c$ for the N−H bond is very similar to other results for symmetrical hydrogen bonds, e.g., Paper 1. Once again, the only major changes on lowering the symmetry of the cation occur around the N···N region. The N−H bond becomes a typical covalent bond (ϱ = 0.313, $\nabla^2\varrho$ = −1.705), and the N···H bond has values typical of a strong hydrogen bond (ϱ = 0.079, $\nabla^2\varrho$ = +0.133). Relative to [4.4.4]H$^+$(i), charge is depleted in the N−C bond to which the proton moves and concentrated in the other N−C bond. The very short N···N distance in [4.4.4]H$^+$(ii) suggests that the hydrogen bond is particularly strong. A comparison of the charge density CP properties for the hydrogen bond CP with those found for the hydrogen bond in $N_2H_7^+$ [9] allows us to further investigate this feature. That study found ϱ = 0.047 and $\nabla^2\varrho$ = +0.096 in a hydrogen bond whose strength was 96 kJ mol^{-1}. Given that Carroll and Bader found strong correlations between hydrogen bond strength and CP properties,[26] it seems safe to conclude that the hydrogen bond in [4.4.4]H$^+$(ii) is considerably stronger than 96 kJ mol^{-1}. (It should be pointed out that the $N_2H_7^+$ study used a different basis set (6-311++G**) to that used here).

Table 6 contains the bond path angle analyses for the free base and [4.4.4]H$^+$(i). The difference between the bond path angle and the geometrical bond path angle $\alpha_b - \alpha_e$ is indicative of the strain at a given atom. The changes in these values on protonation can therefore be used to probe the relief of strain caused by protonation

(22) Bader, R. F. W.; MacDougall, P. J.; Lau, C. D. H. *J. Am. Chem. Soc.* **1984**, *106*, 1594.
(23) Howard, S. T.; Platts, J. A. *J. Phys. Chem.*, in press.
(24) Tang, T.-H.; Hu, W.-J.; Yan, D.-Y.; Cui, Y.-P. *J. Mol. Struct. (THEOCHEM)* **1990**, *207*, 327.
(25) Cioslowski, J. *J. Am. Chem. Soc.* **1992**, *114*, 4382.
(26) Carroll, M. T.; Bader, R. F. W. *Mol. Phys.* **1988**, *65*, 695.

Table 6. Bond Path Angles and Geometric Angles (deg)[a]

	[4.4.4]	[4.4.4]H$^+$(i)	[4.4.4]H$^+$(ii)[b]	N(Me)$_3$	N(Me)$_3$H$^+$
C–N–C	−3.8	−2.9	−3.9, −2.2	−5.4	−0.9
N–N–C	−4.8	−3.1	−4.3, −2.6		
N–C–C	−1.2	−3.0	−2.4, −3.6		
C–C–C	−2.9	−4.1	−4.2, −4.4		

[a] At the 6-31G**//6-31G** level. [b] Results are reported in the form "hydrogen bonding side", "protonated side".

of [4.4.4]. Unlike the geometries and CP results, these show substantial differences between [4.4.4]H$^+$(i) and [4.4.4]H$^+$(ii). Table 6 therefore contains bond path angle results for both cations. The results for [4.4.4]H$^+$(i) suggest some *increase* in strain in the six C–N bonds ($\alpha_b - \alpha_e$ becoming more positive) on protonation, but these are accompanied by *decreases* in strain in the nine C–C bonds. The analagous results for the C_3 cation seem to show that, when the proton is allowed to move away from the central position, a substantial increase in strain occurs at the nitrogen to which the proton moves, accompanied by a decrease in the strain at the other nitrogen.

A major caveat to interpreting the C–N bond results in terms of "strain" is indicated by considering our results for the protonation of trimethylamine and triethylamine (Table 6). In line with Wiberg's findings for NH_3[27] we find the C–N bonds in N(Me)$_3$ are bent "inward", a result of lone pair–bond pair (LP–BP) repulsions. This is also likely to be the reason for the negative ($\alpha_b - \alpha_e$) values found for the C–N bonds in [4.4.4]. The loss of this LP–BP repulsion on protonation causes a positive shift in the ($\alpha_b - \alpha_e$) values; they become less bent. This effect is clearly seen on protonating N(Me)$_3$ (Table 6); so similarly in [4.4.4] we should associate the positive increase in ($\alpha_b - \alpha_e$) at the nitrogen atom on protonation with this loss of LP–BP repulsion, rather than increase in strain. However, these considerations are unimportant for the N–C–C and C–C–C bonds, where we may more safely associate negative shifts in ($\alpha_b - \alpha_e$) with a loss of strain, and indeed this is observed.

Figure 2a–c are maps of $\nabla^2\rho$ for the 6-31G**-optimized [4.4.4], [4.4.4]H$^+$(ii), and N(Et)$_3$, respectively. The plane orientations (see the figure legends) have been chosen to show $\nabla^2\rho$ in the inter N···N regions and also to compare this with N(Et)$_3$ where neither LP–LP repulsion nor hydrogen bonding is present. A comparison of Figures 2a and 2b shows how the charge distribution around the right-hand nitrogen becomes polarized in the direction of the N···H$^+$···N axis when the proton is (asymmetrically) inserted. Since these figures are on the same scale, we may use the width along the N···N axis of the valence shell of charge concentration (VSCC), denoted by the thick black lines where contours are concentrated, to quantify this polarization: a ratio 1.4 is found. We postulate that this is related to the hydrogen bond strength. Comparing Figures 2a and 2c, the charge distribution around the nitrogen LP is apparently almost identical in [4.4.4] and N(Et)$_3$, so it does not appear possible to measure the LP–LP repulsion in the former using the same ideas.

Conclusions

The *ab initio*-optimized structures of the free base [4.4.4] and the D_3-constrained cation [4.4.4]H$^+$(i) are

(27) Wiberg, K. B.; Murcko, M. A. *J. Mol. Struct. (THEOCHEM)* **1988**, *169*, 355.

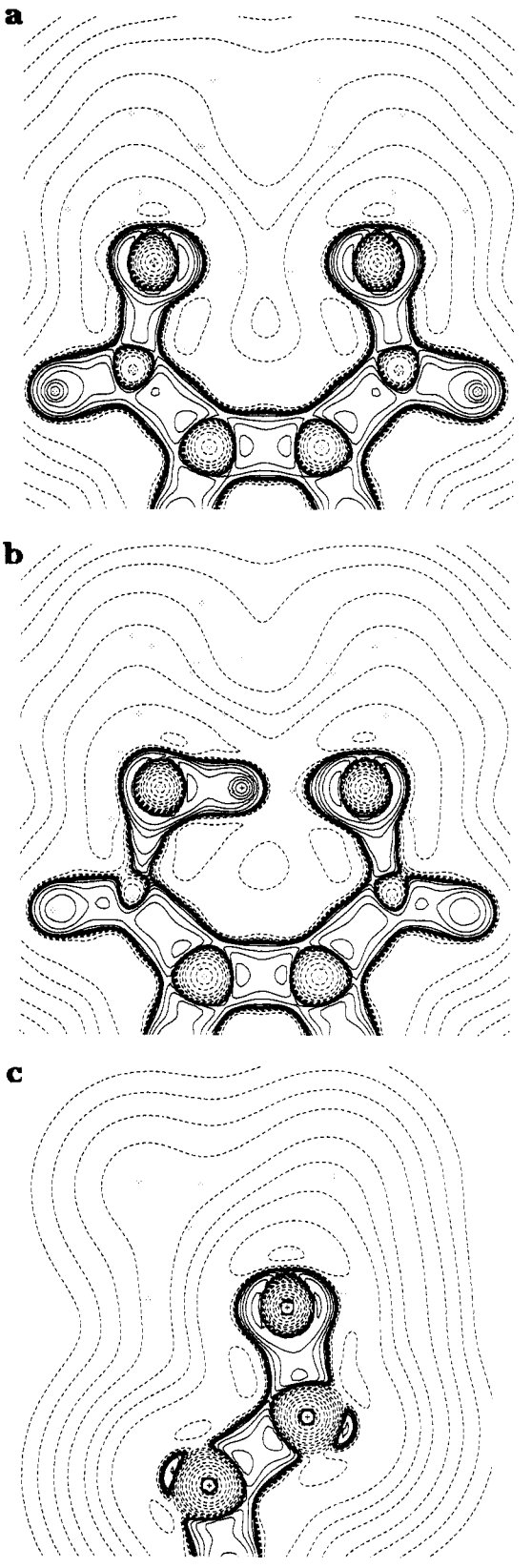

Figure 2. (a) HF/6-31G**//6-31G** $\nabla^2\rho$ distribution for [4.4.4], in the plane containing N1, N1′, and the midpoint of C2 and C2′. Negative contours correspond to the solid lines. Contours plotted at ± 0.002, ± 0.004, ± 0.008, ± 0.02, ± 0.04, ± 0.08, ± 0.2, ± 0.4, ± 0.8, ± 2, ± 4, ± 8, ± 20, ± 40, and ± 80 e Bohr^{-5}. (b) HF/6-31G**//6-31G** $\nabla^2\rho$ distribution for [4.4.4]H$^+$(ii), in the plane containing N1, N1′, and the midpoint of C2 and C2′. Contours as in (a). (c) HF/6-31G**//6-31G** $\nabla^2\rho$ distribution for triethylamine, in the plane containing N1 and the two carbon atoms in one ethyl group. Contours as in (a).

generally in very good agreement with the published crystal structures, except perhaps for the N···N distance in the former which shows a 0.06 Å difference. (In fact, we do not consider this discrepancy to be serious. The STO-3G harmonic frequency calculations reveal several low-frequency $\omega \approx 300$ cm^{-1} normal modes corresponding to "soft" deformations of the DBT cage structure along the N···N axis, i.e., a compression of the cage by some 0.06 Å in the crystal is not unreasonable.) The change in pyramidality of the nitrogen on protonation is somewhat larger in the theoretical calculations, with the angle N1′···N1−C1 showing a 5.1° increase compared to 2.5° for the crystal structures. In agreement with the crystal structure, [4.4.4] has D_3 symmetry, so crystal-packing forces are not responsible for the high symmetry observed in the solid state.

In Paper 1 we established that HF calculations at the 6-31G*//6-31G level predict amine gas phase PAs with an average absolute accuracy of around 0.7%, or typically 6−7 kJ mol^{-1}. The predicted PA for [4.4.4] is computed at a higher level of theory (6-31G**//6-31G**), which was feasible because all calculations could employ at least C_3 symmetry. The main problem for accurate prediction of PAs for molecules of this size is clearly the ZPE correction. (Electron correlation typically changes the electronic energy difference between free base and cation by only 2−5 kJ mol^{-1} [23,28,29] in amines and phosphines, and by 3 kJ mol^{-1} in the $[NH_3···NH_4]^+$ model proton sponge.[8]) The average absolute error in PA at the 6-31G**/6-31G** level for these four monoamines, including ZPE corrections at the 6-31G** level, is about 8 kJ mol^{-1} (with no BSSE corrections). For DBT is was necessary to estimate the 6-31G** ZPE correction by extrapolation using the data in Tables 2 and 3, but a BSSE correction has been included. Taking these factors into account, we estimate the absolute error in our calculated PA is ±10 kJ mol^{-1}.

Asymmetric protonation is energetically preferred by some 11 kJ mol^{-1} at the HF 6-31G**//6-31G** level. High-level calculations on the cationic dimer $[NH_3···NH_4]^+$ [8] suggest that this barrier for proton transfer would be reduced by electron correlation and may be as low as 5−6 kJ mol^{-1}, but the barrier persists; i.e., the PES for for proton transfer is still a double well. Ikuta's correlated calculations on $[NH_3···NH_4]^+$ found an optimum N···N distance some 0.08 Å *smaller* than we find in [4.4.4], so almost certainly a PES for $[NH_3···NH_4]^+$ with the N···N distance fixed at our value of 2.807 Å would still find a double minimum.

Analysis of ϱ and $\nabla^2\varrho$ at the (3,−3) CP shows that, as in DMAN, the very large PA cannot be attributed to an exceptional concentration of charge in the LP and therefore has its origin in the effects such as the proximity of the nitrogens and relief of strain. The bond path analysis of the carbon−carbon bonds supports the hypothesis that strain relief takes place. Comparing bond CPs between $[4.4.4]H^+$ and $N_2H_7^+$ indicates that the nitrogens' proximity, and the resulting hydrogen bond, is an important factor in the high PA of [4.4.4].

Supporting Information Available: Optimized Cartesian coordinates for the free base, $[4.4.4]H^+$(i), and $[4.4.4]H^+$(ii) (3 pages). This material is contained in libraries on microfiche, immediately follows this article in the microfilm version of the journal, and can be ordered from the ACS; see any current masthead page for ordering information.

JO942177F

(28) Dixon, D. A.; Arduengo, A. J. *J. Phys. Chem.* **1991**, *95*, 4180.
(29) Gobbi, A.; Frenking, G. *J. Am. Chem. Soc.* **1993**, *115*, 2362.